Volume 14 | Number 20 | 21 October 2014 | Pages 3897–4106

Lab on a Chip

Miniaturisation for chemistry, physics, biology, materials science and bioengineering

www.rsc.org/loc

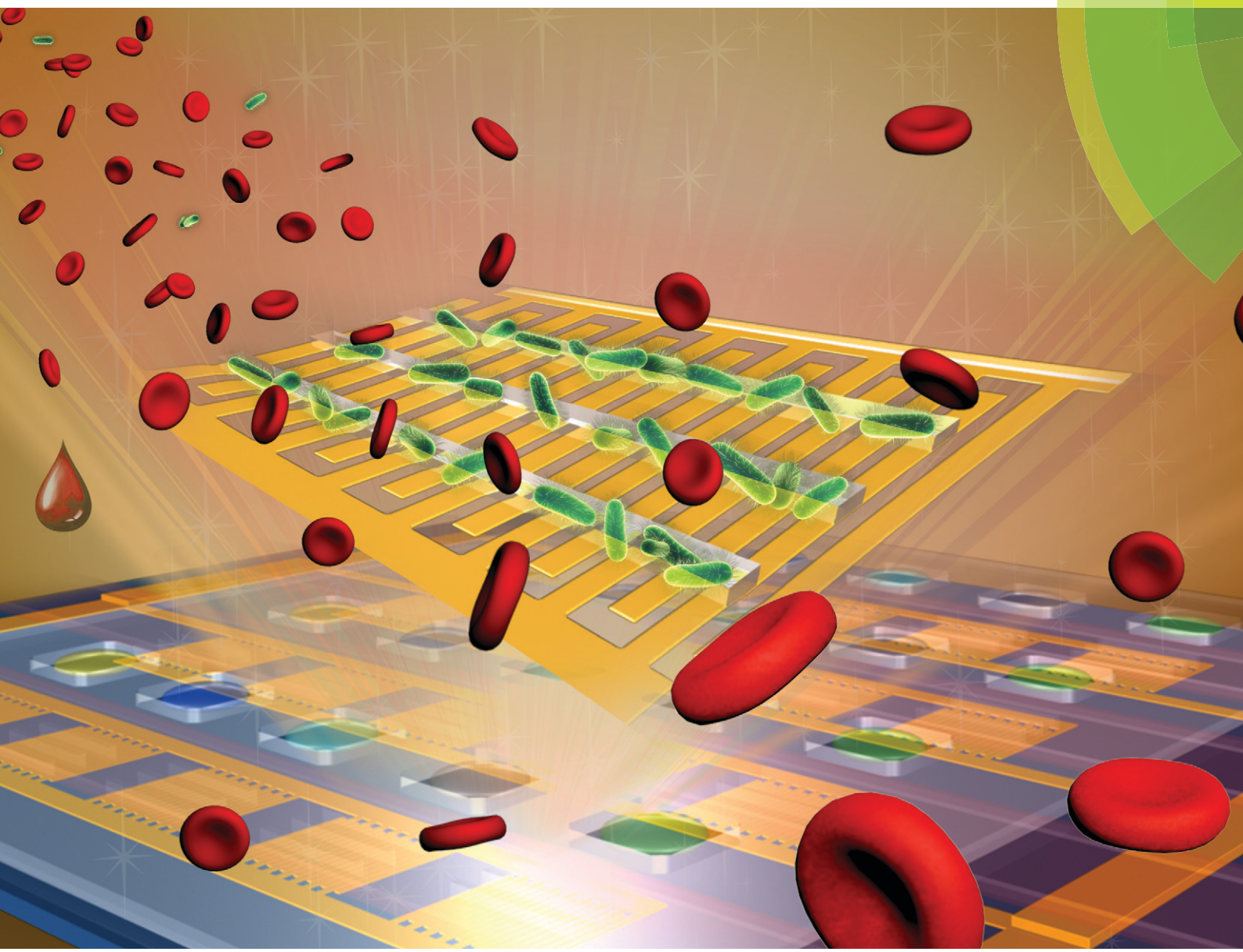

ISSN 1473-0197

ROYAL SOCIETY OF CHEMISTRY

PAPER

Ying-Chun Xu, Wenbin Du *et al.*

An integrated microfluidic device utilizing dielectrophoresis and multiplex array PCR for point-of-care detection of pathogens

Lab on a Chip

PAPER

Cite this: *Lab Chip*, 2014, **14**, 3917

An integrated microfluidic device utilizing dielectrophoresis and multiplex array PCR for point-of-care detection of pathogens†

Dongyang Cai,[ac] Meng Xiao,[b] Peng Xu,[a] Ying-Chun Xu*[b] and Wenbin Du*[ac]

Received 6th June 2014,
Accepted 14th July 2014

DOI: 10.1039/c4lc00669k

www.rsc.org/loc

The early identification of causative pathogens in clinical specimens that require no cultivation is essential for directing evidence-based antimicrobial treatments in resource limited settings. Here, we describe an integrated microfluidic device for the rapid identification of pathogens in complex physiological matrices such as blood. The device was designed and fabricated using SlipChip technologies, which integrated four channels processing independent samples and identifying up to twenty different pathogens. Briefly, diluted whole human blood samples were directly injected into the device for analysis. The pathogens were extracted from the blood by dielectrophoresis, retained in an array of grooves, and identified by multiplex array PCR in nanoliter volumes with end-point fluorescence detection. The universality of the dielectrophoretic separation of pathogens from physiological fluids was evaluated with a panel of clinical isolates covering predominant bacterial and fungal species. Using this system, we simultaneously identified *Pseudomonas aeruginosa*, *Staphylococcus aureus* and *Escherichia coli* O157:H7 within 3 h. In addition to the prompt diagnosis of bloodstream infections, this method may also be utilized for differentiating microorganisms in contaminated water and environmental samples.

Introduction

Bacteria and fungi can enter normally sterile human body sites, such as the peritoneum,[1] blood[2] and cerebrospinal fluid,[3] and cause severe diseases.[4] For example, exogenous bacteria in blood can initiate sepsis, a life-threatening disease killing approximately 24 000 people each day.[2] An accurate and timely diagnosis is one of the major challenges for saving lives from infectious diseases. Currently, culturing samples from the infected sites remains the gold standard for identifying bacterial and fungal infections, and also brings the possibility of determining antibiotic susceptibility.[5] However, current culture-dependent tests are impaired due to the delay in diagnosis and high incidence of false-negative yields. In remote regions, without access to clinical microbiology laboratories, storing and transporting clinical samples will further reduce or delay the yields with positive cultures. Therefore, it is essential to develop new approaches for point-of-care testing (POCT) of infectious diseases.

Extensive research efforts have been made in molecular and other non-culture based methods for addressing the unmet need for early diagnosis of infectious pathogens in clinical samples, including blood.[5] Among various methods, polymerase chain reaction (PCR) is the most sophisticated technique, which amplifies and detects specific nucleic acid sequences from cells, with a potential to speed up the detection of infectious pathogens with very high specificity and sensitivity.[6] However, currently available PCR tests rely on rigorous sample preparation procedures, which prevent them to be used in resource limited settings.

Motivated by further improving the portability and accessibility of POCT, various microfluidic devices, which integrate miniaturized PCR reactors into miniaturized devices, have emerged in recent years.[7–13] However, several important issues have to be addressed before we could practically use these devices. Firstly, clinical samples can be very complex in terms of constituents, and biochemical and rheological properties. For example, one microliter of blood contains 4 to 6 billion erythrocytes and numerous kinds of proteins, but the concentration of bacteria in the early stage of sepsis can be as low as 1 to 100 CFU mL^{-1}. Therefore, the integration of simple, highly efficient and high throughput sample preparation methods on a chip is the key benefit of a

[a] *State Key Laboratory of Microbial Resources, Institute of Microbiology, Chinese Academy of Sciences, 100101 Beijing, China. E-mail: wenbin@im.ac.cn, xycpumch@139.com*
[b] *Department of Clinical Laboratory, Peking Union Medical College Hospital, 100730 Beijing, China*
[c] *Department of Chemistry, Renmin University of China, 100872 Beijing, China*

† Electronic supplementary information (ESI) available: Details of the materials and experiments, PCR primer pairs for detection of pathogens, and figures on device design and optimization are available free of charge *via* the internet. See DOI: 10.1039/c4lc00669k

device-based system compares to conventional PCR techniques.[7] Secondly, most devices have been designed for the specific detection of a single pathogen species in normally sterile clinical samples,[7,14] which is not adequate since a broad range of bacteria and fungi may be present in clinical infectious diseases. A realistic solution to this issue is using multiplex array PCR (maPCR) to identify multiple candidate pathogens simultaneously using an array of PCR reactors.[15] Finally, to develop a system with on-chip sample preparation and maPCR for pathogen identification, an even distribution of isolated pathogens from the sample to all reactors is required, which increases the complexity of the device design and fluidic control.

Dielectrophoresis (DEP)[16] is one of the most widely used approaches among chip-based cell separation methods,[17] providing a selective and label-free separation of particles, such as yeasts,[18] bacteria[19] and viruses.[20] DEP separation of individual pathogen strains from biological samples has recently been performed in microfluidic devices.[21–23] Previous research showed that DEP could be integrated with a PCR microreactor to detect *Listeria monocytogenes* in DI water.[24] Herein, we describe a microfluidic system integrating DEP with chip-based maPCR for the fast separation and identification of pathogens for POCT, as shown in Fig. 1. Whole human blood was used as a model sample to characterize the capability of the system to directly analyze complex physiological fluids. The utility of DEP for broad-spectrum pathogen separation directly from clinical samples, as well as the integration of DEP with maPCR for identifying pathogens have been developed and validated, with the help of recently introduced SlipChip technologies.[25]

Experimental

Fabrication of the microfluidic devices

The microfluidic devices were fabricated with standard photolithography and wet etching techniques.[26] The top plate (2.5 cm × 3 cm) was made of 0.7 mm thick glass with four parallel microchannels (800 μm wide, 15 μm deep), each with five PCR reaction microwells (800 μm × 800 μm in size, 135 μm in depth) evenly distributed on one side. Five additional microwells were made for the negative control as shown in Fig. S1.† The bottom plate (2.5 cm × 4.5 cm) was made of 1 mm thick ITO glass with interdigitated ITO microelectrodes (Fig. 2a). The grooves (the widths varied from 40 μm to 67 μm, the length was 600 μm, and the depth was 5 μm) were fabricated by photolithography of a 5 μm thick SU-8 2005 coating on the bottom plate. The top plate was silanized with dichlorodimethylsilane, while the bottom plate with the ITO electrodes and the SU8 coating was silanized with dimethyldimethoxysilane to make the surface hydrophobic prior to use.

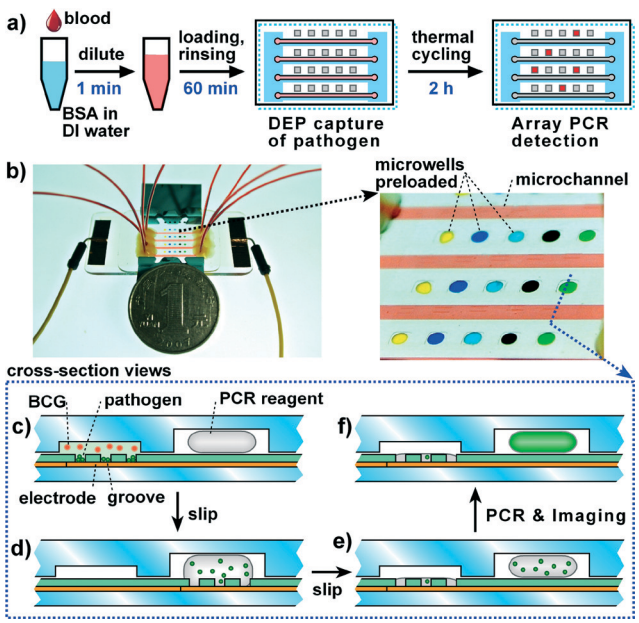

Fig. 1 Device design and operation. a) Diagram depicting the workflow of capturing pathogens from blood and detecting them with multiplex array PCR (maPCR); b) photograph of the device loaded with food dye solutions with a zoomed-in view; c–e) cross-section views of the operation: the water-diluted blood sample, containing blood cell ghosts (BCGs) and pathogens, was loaded into the channel; the pathogens (green dots) were retained in grooves by DEP, while the BCGs were flushed to the outlet; the device was slipped to mix the captured pathogens with preloaded PCR reagents; the top plate was slipped back to its original position and away from the contaminated surfaces; the pathogens were identified by maPCR with fluorescence readout.

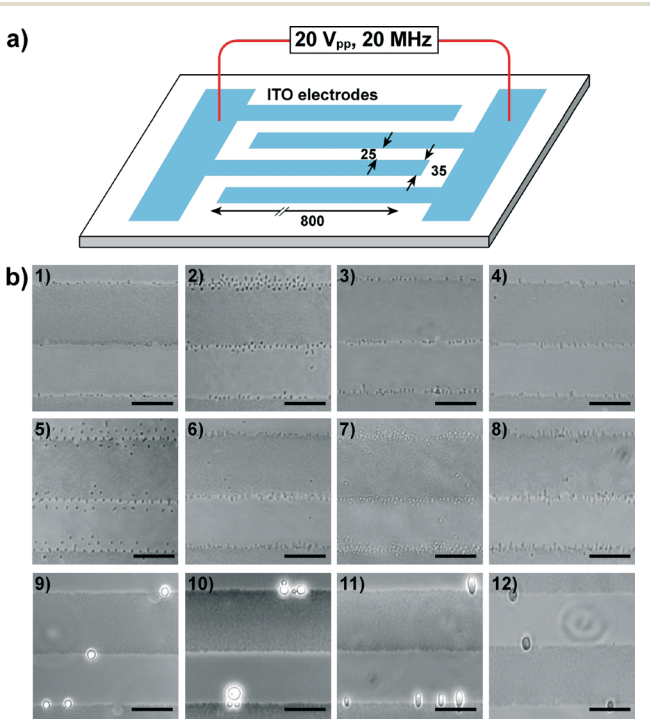

Fig. 2 Dielectrophoresis of various blood-borne pathogens. a) Schematic diagram of the interdigitated ITO microelectrodes; the isolates were deposited onto the electrodes for universality testing; b) the microphotographs show that 12 species of pathogens were captured on the edge of the electrodes by DEP. The isolates were obtained by blood cultures from patients at Peking Union Medical College Hospital (PUMCH). The scale bars are 20 μm.

Preparation of the samples

The original *Escherichia coli* (*E. coli*) strains (RP437 and RP1616) without exogenous plasmids were kindly provided by Professor J. S. Parkinson from the University of Utah. The *E. coli* RP437 carrying plasmid, DsRedT.4, suspended in DI water, was used for optimizing the capture efficiency. The *E. coli* RP1616 carrying plasmid, pAcGFP1 (Clontech), mixed with whole human blood, was used for evaluating the separation efficiency. Four American Type Culture Collection (ATCC) reference strains were used for the evaluation of PCR, namely *E. coli* (ATCC 8739), *E. coli* O157:H7 (ATCC 35150), *Pseudomonas aeruginosa* (*P. aeruginosa*, ATCC 9027) and *Staphylococcus aureus* (*S. aureus*, ATCC 6538p). All bacterial strains were grown in Luria–Bertani (LB) broth and plated on LB agar plates during the log phase growth. Microbial cells were prepared by inoculating 5 mL of LB with a single colony and allowing it to grow overnight at 37 °C. A subculture was prepared in 5 mL of fresh LB and shaken at 37 °C for 5 h. The cells were centrifuged at 8000 g for 5 min and suspended in DI water or diluted blood.

A set of bacterial and fungal clinical isolates, including *E. coli*, *S. aureus*, *P. aeruginosa*, *Klebsiella pneumonia* (*K. pneumonia*), *Acinetobacter baumannii* (*A. baumannii*), *Enterococcus faecium* (*E. faecium*), *Enterococcus faecalis* (*E. faecalis*), *Enterobacter aerogenes* (*E. aerogenes*), *Candida glabrata* (*C. glabrata*), *Candida albicans* (*C. albican*) from positive blood cultures, and two ATCC reference fungal strains namely *Candida krusei* (*C. krusei*) and *Candida parapsilosis* (*C. parapsilosis*), were obtained from the Department of Clinical Laboratory, Peking Union Medical College Hospital (PUMCH, Beijing, China). The name and the serial number of these isolates were listed in the ESI.† All isolates were incubated on blood agar overnight and then adjusted to a 0.5 McFarland standard (approximately 1×10^8 CFU mL^{-1}) with DI water.[27]

Fresh whole human blood was obtained from healthy volunteers at the Hospital of Renmin University of China. The blood was diluted with DI water and microbial cells were added at different final concentrations. The addition of 10 mg mL^{-1} Bovine Albumin Serum (BSA) was used to prevent the adhesion of cells on the microchannel walls. To visualize the blood cell ghosts (BCGs), we stained them with 0.4 mg mL^{-1} rhodamine B. The concentration of the BCGs in the original blood sample was roughly 4×10^9 cells mL^{-1}.

Device assembly

The bottom plate was placed in a 9 cm Petri dish, with the patterned side facing up. 10 mL de-gassed mineral oil was poured into the Petri dish to cover the bottom plate. 50 nL of the PCR mixture with different primer pairs was deposited into each microwell as described previously.[15,25] The top plate was carefully placed onto the bottom plate, with the microchannels aligned with the grooves on the bottom plate (Fig. 1b). The two halves of the device were secured by two small binder clips.

DEP separation of the microbial cells from blood

Four 250 μL syringes (Agilent, Santa Clara, CA) with 30-gauge Teflon tubing (Zeus Inc., Orangeburg, SC) were connected with the microchannels *via* access holes and sealed with capillary wax (Hampton, Aliso Viejo, CA). The samples were fed into the microchannels at a flow rate of 1 μL min^{-1}, unless declared otherwise. The microbial cells were captured in the grooves when a high frequency alternating current (HFAC) signal of 20 V_{pp} (peak-to-peak voltage) and 20 MHz was applied between the interdigitated microelectrodes. The concentrations of the microbial cells in the samples before and after DEP were determined by fluorescence imaging using an Eclipse Ti inversed microscope (Nikon, Japan), equipped with a CoolSNAP HQ2 CCD camera (Photometrics, Tucson, AZ). After capturing, the grooves with the captured microbial cells were flushed with DI water at a flow rate of 2 μL min^{-1} for 10 min to remove the PCR inhibitors.

maPCR identification of the pathogens

PCR was performed in an Eppendorf Mastercycler with an *in situ* Adapter (Hamburg, Germany). The initial step, to lyse the bacteria and activate the enzyme for reaction, was carried out for 10 min at 95 °C. Next, a total of 30 cycles of amplification was performed as follows: a DNA denaturation step of 15 s at 95 °C; a primer annealing step and DNA extension step of 50 s at 65 °C. After the final cycle, a DNA extension step was performed for 5 min at 72 °C. A final hold temperature of 4 °C was utilized to deactivate the enzyme.

Ethics statement

The study was approved by the Hospital of Renmin University China Ethics Board and the Committee and Research Ethics Board of PUMCH. All volunteer blood donors and all patients related to blood culture isolates provided informed consent.

Results and discussion

The design and operation of the microfluidic device

One of our primary objectives is to establish a broad-spectrum microbial isolation method compatible with clinical samples, using blood as the model sample. To prevent false positive results due to the existence of circulating microbial DNA (DNAemia) and avoid DNA loss during extraction,[28] it is desirable to develop a device which directly captures pathogen cells from blood and detects them afterwards. DEP was previously used as a selective separation method for different microorganisms.[19] Here, by choosing appropriate parameters, DEP was validated as a broad-spectrum capture method for major bloodstream infection (BSI)-causing microbial species. Subsequently, our efforts were directed towards incorporating DEP as the capture module for on-chip PCR, thus the DEP-captured microbial cells could be identified by PCR amplification with corresponding primer pairs. To identify causative pathogens in BSIs, we introduced an array design of a DEP–PCR integration in a 4 × 5 matrix, which was realized

by SlipChip technologies.[25] As a difference from previously reported SlipChip devices, which use pipettes to inject microliter samples or reagents into the microwells, in this work, we designed a device which was able to process blood samples continuously to allow the enrichment of pathogen cells from a large volume of samples. The operation of the device is shown in Fig. 1. Samples were injected into the channels at a constant flow rate. Facilitated by positive DEP force, the microbial cells were captured in the grooves. Then, DI water was loaded to rinse off the PCR inhibitors as well as other interfering components in the samples. The device was then slipped to overlay the grooves containing the microbial cells on the bottom plate with the microwells preloaded with PCR reagents on the top plate. As the HFAC on the electrodes was removed, the microbial cells were released and dispersed into the PCR reagents. When the top plate was slipped back, the device was placed on a standard thermal cycler for PCR amplification and the results were obtained by imaging with the microscope. It took approximately 3 h from sample loading to detection.

Broad-spectrum pathogen capture with DEP

To evaluate if DEP could capture a broad-spectrum of pathogen species, we tested a variety of bacteria and fungi isolates from BSIs with our DEP capture electrodes (Fig. 2). Interdigital electrodes (900 μm long, 35 μm wide with 25 μm spacing) were designed for the highly efficient DEP capture, as shown in Fig. 2a. During the experiment, the sample was deposited on the electrodes and the HFAC was applied between the interdigitated microelectrodes. 34 clinical isolates were selected based on the ranking of predominant species causing BSIs (see Table 1 and the ESI†).[29] According to the Peking Union Medical College Hospital (PUMCH) surveillance data obtained from positive blood cultures from January 2008 to December 2012, these isolates covered 70.3% of pathogen species other than coagulase-negative *staphylococci* (which are the most common contaminants of BC).[30] To further verify the applicability of our system for candidemia diagnosis,[31] we tested another two reference fungal strains with high incidence of infection. As shown in Fig. 2b, all isolates, from 0.8 μm-sized *S. aureus* to 5 μm-sized *C. albican*, were attracted to the edge of the electrodes under the same conditions (20 V_{pp}, 20 MHz). The captured pathogens were visualized under the microscope for optical inspection of the pathogen morphologies.[32] Our primary experiments also showed that it could also capture bacteria from milk or other physiological fluids after dilution (results not shown). In consideration of the representativeness of the isolates we have tested, we believe that DEP can be qualified as a broad-spectrum pathogen enrichment method for clinical samples.

In this work, the planar electrodes on the bottom plate were used for simplicity of fabrication. However, the DEP force acting on the microbial cells rapidly decreased when it moved away from the plane of the electrodes. This limited the depth of the loading channel we could design (15 μm) and consequently affected the throughput of sample processing. To solve this problem, three dimensional dielectrophoretic electrodes, which could provide a better trapping efficiency and processing throughput, could be used.[33,34] This will enable us to further decrease the limit of detection for rare pathogens in clinical samples.

Table 1 Pathogens captured by DEP shown in Fig. 2

	Name	Serial number	Category	Rate[a]
1	*S. aureus*	13B01049	Gram-positive	10%
2	*E. aerogenes*	13B02461	Gram-negative	N/A
3	*E. faecium*	13B01945	Gram-positive	4%
4	*E. faecalis*	13B00767	Gram-positive	4%
5	*K. pneumoniae*	13B00139	Gram-negative	9%
6	*E. coli*	13B00431	Gram-negative	18%
7	*A. baumannii*	13B02045	Gram-negative	7%
8	*P. aeruginosa*	13B00286	Gram-negative	3%
9	*C. glabrata*	13H04036	Fungi	N/A
10	*C. albicans*	13Z17401	Fungi	2%
11	*C. krusei*	ATCC 6258	Fungi	N/A
12	*C. parapsilosis*	ATCC 22019	Fungi	1%

[a] The rates of infection were provided by the PUMCH surveillance data obtained from positive blood cultures.

Design and optimization of the grooves

As shown in Fig. 3, three capture grooves were fabricated for each capture unit. The grooves were designed to be narrower than the loading channel and were arranged in a ladder-like layout so that each unit only captured pathogen cells from a part of the sample flowing through the channel. Compared to designs with only one capture groove in each unit, dividing it into three grooves in each unit and evenly distributing them across the microchannel helped to reduce an unequal capture ratio, caused by a flow rate difference of the parabolic flow.

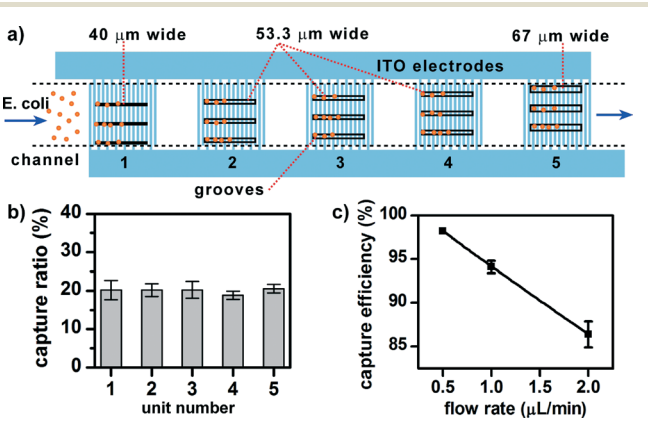

Fig. 3 Efficiency and distribution of the DEP-capture of the bacteria (*E. coli*) using units of grooves. a) Schematic diagram of the bacteria captured by DEP in the grooves with optimized widths; each capture unit had 3 capture grooves with the same width; the widths for unit 1, unit 2–4 and unit 5 were 40 μm, 53.3 μm and 67 μm, respectively; b) equal distribution of captured *E. coli* cells in the five units with optimized groove widths; c) the effect of the flow rate on the overall capture efficiency.

The grooves had a depth of 5 μm for retaining bacterial or fungal cells during slipping.

The geometry of the grooves was optimized with RFP-tagged *E. coli* RP437 cells at a concentration of ~2 × 10^5 CFU mL^{-1}, a flow rate of 1 μL min^{-1} and a capture time of 10 min. Under these conditions, microbial cells captured in the grooves did not overlap and could be counted with fluorescence imaging. We initially designed 15 grooves with an individual width of 53.3 μm (800/15) in the five units. As shown in Fig. S2d,† the capture ratio of the five units along the channel was around 4 : 2 : 2 : 2 : 1. The capture ratio of units 2, 3 and 4 was about 1/5 and unit 1 captured more bacteria than its width could cover, resulting in fewer cells captured by unit 5. This indicated that preceding grooves affected the capture efficiency of the latter. Therefore, we optimized the design. The width of the grooves in unit 1 was reduced. Units 2, 3 and 4 remained unchanged, and the groove width of unit 5 was increased. In the optimal design, the groove width of unit 1 was 40 μm and that of unit 5 was 67 μm. A uniform capture ratio of the RFP-tagged *E. coli* RP437 for the five units was obtained, as shown in Fig. 3b. All of the experiments were repeated three times.

To evaluate the capture efficiency of the device, we monitored the concentration change of the microbial cells in the samples before and after the DEP capture. Before the grooves were saturated by the *E. coli* cells, we took one microphotograph at the upstream and another at the downstream (repeated 5 times). The cell number in each image was counted to calculate the DEP capture efficiency. At a flow rate of 1 μL min^{-1}, a capture efficiency of 94.1% was attained, as shown in Fig. 3c.

Isolation of the pathogens from the blood samples

To demonstrate the successful isolation of the pathogens from the complex physiological fluids, blood samples containing ~1.6 × 10^7 CFU mL^{-1} GFP-tagged *E. coli* RP1616 cells were used and diluted with DI water before being loaded into the channel. The fluorescence images, shown in Fig 4, were obtained using 100-fold diluted blood. Before the DEP capture, the overlay of green fluorescence and red fluorescence channels showed the coexistence of GFP-tagged *E. coli* with BCGs (Fig. 4b). By applying the HFAC on the ITO electrodes, the *E. coli* cells were captured in the grooves by positive DEP force (Fig. 4c) and the BCGs, which received a negative DEP force, were carried away by the flow to the outlets (Fig. 4d). Here, we found that the capture efficiency of DEP was affected by the conductivity of the sample. For 10-fold and 100-fold dilutions, the conductivity of the blood reduced to 1.07 mS cm^{-1} and 0.15 mS cm^{-1} (22 °C), while the capture efficiency increased to 70.9% and 91.5%, respectively (Fig. 4e). *E. coli* RP1616 cells suspended in DI water were used as a control sample, for which the highest capture efficiency, 94.8%, was obtained. All of the experiments were replicated three times.

Elimination of contaminants before PCR

To eliminate the contaminating components from whole human blood, we first rinsed the captured microbial cells for 10 min at a flow rate of 2 μL min^{-1}. After the DEP capture, we slipped the top plate to overlap the PCR mixture with the grooves. We discovered that after PCR, the droplet shape was irregular and sometimes a serious leakage of PCR reagents occurred. We speculated that the surfaces of the grooves and ITO electrodes were contaminated during sample loading, which made it hydrophilic. To overcome this problem, we simply slipped back the top plate to its original position and moved the droplets of the PCR mixture away from the contaminated surfaces (Fig. 5a–d). This allowed us to get uniform droplet shapes and a better PCR efficiency, indicated by a higher intensity of fluorescence shown in Fig. 5e and f.

Performance of maPCR

To evaluate the performance of array PCR on our device for the fast identification of pathogens, we loaded a 100-fold diluted blood sample into the channel, containing 1.6 × 10^3 CFU mL^{-1} *E. coli* 8739. Meanwhile, every microwell on the top plate was pre-loaded with a 50 nL droplet composed of the PCR master mixture and primers targeting the LacZ gene.[38] As shown in

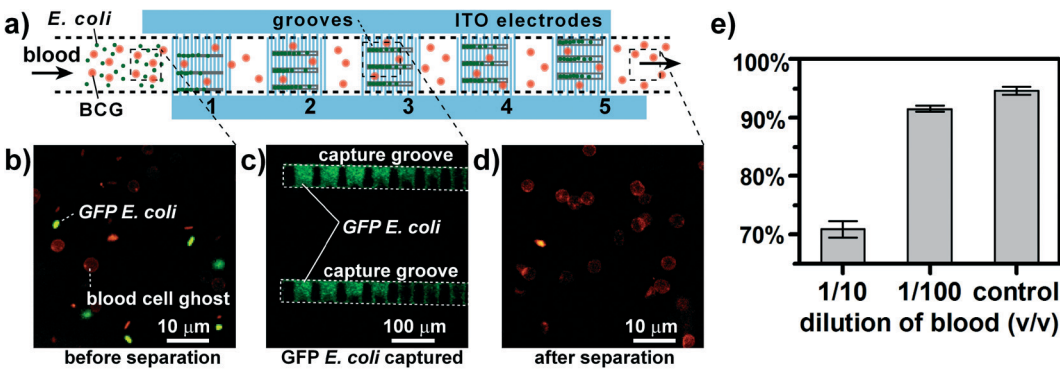

Fig. 4 Separation of *E. coli* cells from whole human blood by DEP. a) Schematic diagram showing one channel during separation; b) at the up-stream of the channel before DEP capture, BCGs (red) coexisted with a large amount of *E. coli* (green); c) DEP capture of *E. coli* in the grooves from the sample (flow rate: 1 μL min^{-1}); d) at the downstream of the channel after DEP capture, the concentration of the BCGs stayed the same as before the process, but *E. coli* were almost eliminated; e) the effect of blood dilution on the capture efficiency of *E. coli* from blood.

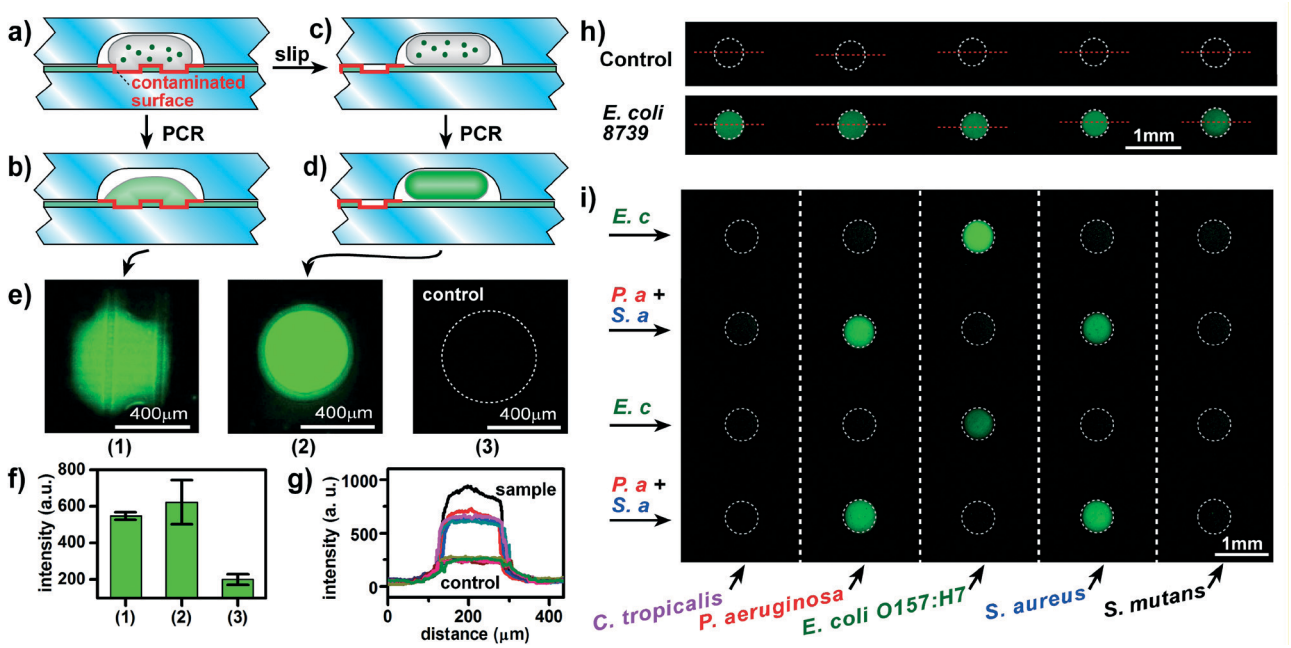

Fig. 5 a–d) Schematic diagrams of the slipping procedure before initiating PCR. The top plate was slipped back to avoid the microwell, containing the PCR mixture and *E. coli* cells, to overlay with the contaminated surface during PCR; e) microphotographs of the PCR droplets on/off the capture electrodes and a control droplet without *E. coli*; f) the average fluorescence intensity of the droplets in panel e; g) the average fluorescence intensity of the droplets in panel h; h) montages of fluorescence microphotographs show the detection of DEP-captured *E. coli* by on-chip PCR, compared to the control with no *E. coli*; i) montages of fluorescence microphotographs show the identification of different pathogens in four samples with maPCR.

Fig. 5h, the control microwells overlaid with the grooves without *E. coli* showed no increase in fluorescence, while those overlaid with the grooves containing the captured *E. coli* showed a significant increase in fluorescence intensity after thermal cycling. Line scans across the middle of the individual microwells, shown in the top and bottom panels of Fig. 5h, showed that the average fluorescence intensity of the microwells containing the *E. coli* 8739 cells was more than 2-fold higher than that of the control ($p < 0.0001$, $n = 5$) (Fig. 5g). No cross-contamination occurred among the adjacent channels and the results were reproducible.

Validation of the method with blood samples

To demonstrate the capability of the device for identifying candidate pathogens in multiple samples, we preloaded the microwell array with five different primer pairs targeting dominating pathogens of BSIs, namely *Candida tropicalis* (*C. tropicalis*), *P. aeruginosa*, *E. coli* O157:H7, *S. aureus* and *Streptococcus mutans* (*S. mutans*) (see Table S1 in the ESI† for the primer design). It has been reported that more than 90% of cases of BSIs were infected by a single pathogenic species.[35] Therefore, model blood samples containing one or two pathogens were tested. Sample 1 was loaded into channels 1 and 3, containing 1.8×10^3 CFU mL^{-1} *E. coli* O157:H7 only; sample 2 was loaded into channels 2 and 4, containing a mixture of 1.0×10^3 CFU mL^{-1} *P. aeruginosa* (ATCC 9027) and 2.3×10^3 CFU mL^{-1} *S. aureus* (ATCC 6538p). After 50 minutes sampling, 10 minutes rinsing and 2 h PCR amplification, the PCR results were measured, shown in Fig. 5i. Only the microwells preloaded with primer pairs targeting the corresponding pathogens showed a significant increase in fluorescence intensity, indicating a high specificity and reproducibility of the system.

Conclusions

The direct detection of pathogens in clinical samples is challenging for low concentrations of pathogens and the vast diversity and complexity of the samples. In this work, we developed a simple and portable microfluidic device for pathogen separation and identification in complex samples such as whole human blood. With grooves in a ladder-like layout over DEP electrodes, the device efficiently and uniformly isolated pathogens from a model sample in an array containing 40 000 times more blood cells. With simple slipping operations, the captured pathogens were mixed with an array of nanoliter reagents for PCR identification of up to twenty pathogens simultaneously. The device can detect pathogens with a concentration in the order of ~10^3 CFU mL^{-1}.

In comparison to conventional culture-based methods, which take at least 24 to 72 h, the device can detect pathogens within three hours from sample-in to answer-out. By optimizing the PCR conditions, the time might be further reduced to less than 1.5 h.[7] Dielectrophoresis was found to be a universal sample preparation method for capturing broad-spectrum

pathogens. The usefulness of DEP separation was manifested after we coupled it with maPCR, enabling a simultaneous identification of multiple candidate pathogens. Additionally, this design may be adopted for other assays based on preloaded reagents with nanoliter volumes. In an ongoing work, we are exploiting this array design with multiple antibiotics to screen the antibiotic resistance of captured pathogens. This DEP–maPCR system provided a convenient and accessible approach for early diagnosis of infectious diseases caused by bacteria and fungi, greatly simplifying sample preparation procedures and eliminating contamination during PCR with preloaded reagents. We are convinced that this system can also be adopted for other applications such as food safety testing, water quality analysis and assessment of microbial communities in the environment.

Future work will be directed towards improving the throughput of the sample processing, expanding the array size to increase the coverage, and optimizing the performance of amplification using PCR or Loop-Mediated Isothermal Amplification (LAMP),[36] to further reduce the limit of detection. Moreover, portable DEP power supplies, thermal cyclers,[37,38] self-containing microflow control systems,[39,40] and smartphone-based imaging[41,42] could be incorporated to make the system more compact and portable in resource limited conditions.

Acknowledgements

This study is supported by the State key Laboratory of Microbial Resources, Institute of Microbiology, Chinese Academy of Sciences (SKLMR-20120604); the National Natural Science Foundation of China (21205134, 31230003 and 201402001) and the program of China Ocean Mineral Resources R&D Association (grant DY125-15-R-02).

Notes and references

1 B. Appenrodt, F. Grunhage, M. G. Gentemann, L. Thyssen, T. Sauerbruch and F. Lammert, *Hepatology*, 2010, **51**, 1327–1333.
2 K. Reinhart, R. Daniels, N. Kissoon, J. O'Brien, F. R. Machado and E. Jimenez, *J. Crit. Care*, 2013, **28**, 526–528.
3 M. C. Thigpen, C. G. Whitney, N. E. Messonnier, E. R. Zell, R. Lynfield, J. L. Hadler, L. H. Harrison, M. M. Farley, A. Reingold, N. M. Bennett, A. S. Craig, W. Schaffner, A. Thomas, M. M. Lewis, E. Scallan and A. Schuchat, *N. Engl. J. Med.*, 2011, **364**, 2016–2025.
4 P. Cossart and P. J. Sansonetti, *Science*, 2004, **304**, 242–248.
5 K. Reinhart, M. Bauer, N. C. Riedemann and C. S. Hartog, *Clin. Microbiol. Rev.*, 2012, **25**, 609–634.
6 J. P. Casalta, F. Gouriet, V. Roux, F. Thuny, G. Habib and D. Raoult, *Eur. J. Clin. Microbiol. Infect. Dis.*, 2009, **28**, 569–573.
7 C. J. Easley, J. M. Karlinsey, J. M. Bienvenue, L. A. Legendre, M. G. Roper, S. H. Feldman, M. A. Hughes, E. L. Hewlett, T. J. Merkel, J. P. Ferrance and J. P. Landers, *Proc. Natl. Acad. Sci. U. S. A.*, 2006, **103**, 19272–19277.
8 J. Pipper, Y. Zhang, P. Neuzil and T. Hsieh, *Angew. Chem., Int. Ed.*, 2008, **47**, 3900–3904.
9 M. Liong, A. N. Hoang, J. Chung, N. Gural, C. B. Ford, C. Min, R. R. Shah, R. Ahmad, M. Fernandez-Suarez, S. M. Fortune, M. Toner, H. Lee and R. Weissleder, *Nat. Commun.*, 2013, **4**, 1752.
10 H. J. Chung, C. M. Castro, H. Im, H. Lee and R. Weissleder, *Nat. Nanotechnol.*, 2013, **8**, 369–375.
11 P. Yager, T. Edwards, E. Fu, K. Helton, K. Nelson, M. R. Tam and B. H. Weigl, *Nature*, 2006, **442**, 412–418.
12 C. Zhang and D. Xing, *Nucleic Acids Res.*, 2007, **35**, 4223–4237.
13 A. M. Foudeh, D. T. Fatanat, T. Veres and M. Tabrizian, *Lab Chip*, 2012, **12**, 3249–3266.
14 M. Liong, A. N. Hoang, J. Chung, N. Gural, C. B. Ford, C. Min, R. R. Shah, R. Ahmad, M. Fernandez-Suarez, S. M. Fortune, M. Toner, H. Lee and R. Weissleder, *Nat. Commun.*, 2013, **4**, 1752.
15 F. Shen, W. B. Du, E. K. Davydova, M. A. Karymov, J. Pandey and R. F. Ismagilov, *Anal. Chem.*, 2010, **82**, 4606–4612.
16 H. A. Pohl, *J. Appl. Phys.*, 1958, **29**, 1182–1188.
17 B. Cetin and D. Li, *Electrophoresis*, 2011, **322**, 410–427.
18 M. C. Jaramillo, R. Martinez-Duarte, M. Huttener, P. Renaud, E. Torrents and A. Juarez, *Biosens. Bioelectron.*, 2013, **43**, 297–303.
19 J. Cheng, E. L. Sheldon, L. Wu, A. Uribe, L. O. Gerrue, J. Carrino, M. J. Heller and J. P. O'Connell, *Nat. Biotechnol.*, 1998, **16**, 541–546.
20 N. G. Green, H. Morgan and J. J. Milner, *J. Biochem. Biophys. Methods*, 1997, **35**, 89–102.
21 I. F. Cheng, V. E. Froude, Y. X. Zhu, H. C. Chang and H. C. Chang, *Lab Chip*, 2009, **9**, 3193–3201.
22 R. S. Kuczenski, H. C. Chang and A. Revzin, *Biomicrofluidics*, 2011, **5**, 32005–3200515.
23 U. C. Schroder, A. Ramoji, U. Glaser, S. Sachse, C. Leiterer, A. Csaki, U. Hubner, W. Fritzsche, W. Pfister, M. Bauer, J. Popp and U. Neugebauer, *Anal. Chem.*, 2013, **85**, 10717–10724.
24 S. Bhattacharya, S. Salamat, D. Morisette, P. Banada, D. Akin, Y. S. Liu, A. K. Bhunia, M. Ladisch and R. Bashir, *Lab Chip*, 2008, **8**, 1130–1136.
25 W. Du, L. Li, K. P. Nichols and R. F. Ismagilov, *Lab Chip*, 2009, **9**, 2286–2292.
26 Q. H. He, S. Chen, Y. Su, Q. Fang and H. W. Chen, *Anal. Chim. Acta*, 2008, **628**, 1–8.
27 *Performance Standards for Antimicrobial Susceptibility Testing*, 23rd Informational Supplement M100-S23, Clinical and Laboratory Standards Institute, Wayne, PA, USA, 2013.
28 P. L. White, M. D. Perry, J. Loeffler, W. Melchers, L. Klingspor, S. Bretagne, E. McCulloch, M. Cuenca-Estrella, N. Finnstrom, J. P. Donnelly and R. A. Barnes, *J. Clin. Microbiol.*, 2010, **48**, 3753–3755.
29 A. Kumar, D. Roberts, K. E. Wood, B. Light, J. E. Parrillo, S. Sharma, R. Suppes, D. Feinstein, S. Zanotti, L. Taiberg, D. Gurka, A. Kumar and M. Cheang, *Crit. Care Med.*, 2006, **34**, 1589–1596.
30 S. E. Beekmann, D. J. Diekema and G. V. Doern, *Infect. Control Hosp. Epidemiol.*, 2005, **26**, 559–566.

31 K. W. Garey, M. Rege, M. P. Pai, D. E. Mingo, K. J. Suda, R. S. Turpin and D. T. Bearden, *Clin. Infect. Dis.*, 2006, **43**, 25–31.
32 R. M. Cooper, D. C. Leslie, K. Domansky, A. Jain, C. Yung, M. Cho, S. Workman, M. Super and D. E. Ingber, *Lab Chip*, 2014, **14**, 182–188.
33 J. Voldman, M. Toner, M. L. Gray and M. A. Schmidt, *J. Electrost.*, 2003, **57**, 69–90.
34 Y. Xu, H. Yao, L. Wang, W. Xing and J. Cheng, *Lab Chip*, 2011, **11**, 2417–2423.
35 N. Wellinghausen, A. J. Kochem, C. Disque, H. Muhl, S. Gebert, J. Winter, J. Matten and S. G. Sakka, *J. Clin. Microbiol.*, 2009, **47**, 2759–2765.
36 F. B. Myers, R. H. Henrikson, J. Bone and L. P. Lee, *PLoS One*, 2013, **8**, e70266.
37 J. Pipper, Y. Zhang, P. Neuzil and T. M. Hsieh, *Angew. Chem., Int. Ed.*, 2008, **47**, 3900–3904.
38 J. Wang, Z. Y. Chen, P. Corstjens, M. G. Mauk and H. H. Bau, *Lab Chip*, 2006, **6**, 46–53.
39 W. B. Du, Q. Fang, Q. H. He and Z. L. Fang, *Anal. Chem.*, 2005, **77**, 1330–1337.
40 I. You, S. M. Kang, S. Lee, Y. O. Cho, J. B. Kim, S. B. Lee, Y. S. Nam and H. Lee, *Angew. Chem., Int. Ed.*, 2012, **51**, 6126–6130.
41 I. Navruz, A. F. Coskun, J. Wong, S. Mohammad, D. Tseng, R. Nagi, S. Phillips and A. Ozcan, *Lab Chip*, 2013, **13**, 4015–4023.
42 D. Witters, B. Sun, S. Begolo, J. Rodriguez-Manzano, W. Robles and R. F. Ismagilov, *Lab Chip*, 2014, DOI: 10.1039/C4LC00248B.

